Supplementary Information

Lanthanide ion-doped silica nanohelix:
a helical inorganic network acts as a chiral source for metal ions

Tomoyuki Harada,[a] Hiroshi Yanagita,[a] Naoya Ryu,*[b] Yutaka Okazaki,[c] Yutaka Kuwahara,[a]
Makoto Takafuji,[a] Shoji Nagaoka,[ab] Hirotaka Ihara *[a] and Reiko Oda *[d]

[a.] *Department of Applied Chemistry and Biochemistry, Kumamoto University*
2-39-1 Kurokami, Chuo-ku Kumamoto 860-8555 (Japan)

[b.] *Materials Development Department, Kumamoto Industrial Research Institute*
3-11-38 Higashimachi, Higashi-ku Kumamoto 862-0901 (Japan)

[c.] *International Research and Education Centre of Advanced Energy Science,*
Graduate School of Energy Science, Kyoto University
Yoshida-Honmachi, Sakyo-ku Kyoto 606-8501 (Japan)

[d.] *Institut de Chimie & Biologie des Membranes & des Nano-objets (UMR5248 CBMN), CNRS,*
Université de Bordeaux, Institut Polytechnique Bordeaux
2 rue Robert Escarpit, 33607 Pessac (France)

n-ryu@kumamoto-iri.jp / ihara@kumamoto-u.ac.jp / reiko.oda@u-bordeaux.fr

Experimental details

Materials

The cationic gemini surfactants with enantiomeric tartrate counterions (16-2-16 L- and D-tartrate) were synthesized according to the previously reported procedure.[12] Other chemicals were purchased from chemical suppliers and used without further purification. Millipore deionized water was used throughout this work.

Structure confirmation

The chemical structures of the gemini surfactants were confirmed by Fourier transform infrared spectroscopy (FTIR) measurements with a JASCO FT/IR-6300 FTIR spectrometer equipped with a JASCO ATR Pro450-S, proton nuclear magnetic resonance spectroscopy (^{1}H NMR) measurements with a JEOL JNM-ECZ400R NMR spectrometer and elemental analysis (EA) with an Elementar vario MICRO cube elemental analyser.

N,*N′*-Dihexadecyl-*N*,*N*,*N′*,*N′*-tetramethylethylene diammonium L-tartrate (16-2-16 L-tartrate): White solid; FTIR (ATR): 3372, 2955, 2917, 2850, 1606, 1468, 1349 and 719 cm^{-1}; ^{1}H NMR (400 MHz, CD_3OD): δ 0.90 (6 H, t, J = 6.9 Hz, $CH_3CH_2 \times 2$), 1.29 (48 H, s, $CH_3(CH_2)_{12} \times 2$), 1.41–1.42 (4 H, m, $CH_3(CH_2)_{12}CH_2 \times 2$), 1.80–1.84 (4 H, m, $CH_3(CH_2)_{13}CH_2 \times 2$), 3.20 (12 H, s, $N^+(CH_3)_2 \times 2$), 3.41 (4 H, m, $CH_3(CH_2)_{14}CH_2 \times 2$), 3.92 (4 H, s, $N^+(CH_2)_2N^+$), 4.32 (2 H, s, $(CH)_2$) ppm; EA: (Found: C, 67.12; H, 11.70; N, 3.62%. Calculated for $C_{42}H_{86}N_2O_2 \cdot 2.0H_2O$: C, 67.15; H, 12.08; N, 3.73%).

N,*N′*-Dihexadecyl-*N*,*N*,*N′*,*N′*-tetramethylethylene diammonium D-tartrate (16-2-16 D-tartrate): White solid; FTIR (ATR): 3375, 2955, 2918, 2850, 1606, 1468, 1348 and 719 cm^{-1}; ^{1}H NMR (400 MHz, CD_3OD): δ 0.90 (6 H, t, J = 6.8 Hz, $CH_3CH_2 \times 2$), 1.29 (48 H, s, $CH_3(CH_2)_{12} \times 2$), 1.41–1.42 (4 H, m, $CH_3(CH_2)_{12}CH_2 \times 2$), 1.79–1.84 (4 H, m, $CH_3(CH_2)_{13}CH_2 \times 2$), 3.21 (12 H, s, $N^+(CH_3)_2 \times 2$), 3.42 (4 H, m, $CH_3(CH_2)_{14}CH_2 \times 2$), 3.93 (4 H, s, $N^+(CH_2)_2N^+$), 4.32 (2 H, s, $(CH)_2$) ppm; EA: (Found: C, 66.96; H, 11.72; N, 3.60%. Calculated for $C_{42}H_{86}N_2O_2 \cdot 2.2H_2O$: C, 66.83; H, 12.07; N, 3.71%).

Preparation of helical and twisted silica nanoribbons

16-2-16 L- or D-tartrate was dissolved at 60 °C (3.0 mM, 20 mL) and then cooled at 20 °C for 24 h. 16-2-16 L-tartrate formed exclusively right-handed helices (Fig. S1a), and its enantiomer, 16-2-16 D-tartrate, formed left-handed ones (Fig. S1b). To the 16-2-16 tartrate aqueous dispersion, tetraethyl orthosilicate (TEOS) aqueous solution (TEOS:water = 1:10 v/v, 20 mL) containing the corresponding enantiomer of tartaric acid (0.2 mM) was added and then kept at 20 °C for 18 h. The resulting precipitate after the polycondensation of TEOS was thoroughly washed with hot methanol (about 55 °C) to remove the organic 16-2-16 self-assemblies as well as unreacted excess of TEOS. The remained amount of the template was negligible, which was estimated to be <1 wt% by elemental analysis (below the detection limit).[12] Twisted silica nanoribbons were obtained with 1.5 h aging time of 16-2-16 tartrate aqueous dispersion.

Scanning transmission electron microscopy observation and energy dispersive X-ray spectral measurement

Scanning transmission electron microscopy (STEM) observation and energy dispersive X-ray spectral (EDX) measurement were made with a HITACHI SU8000 scanning electron microscope equipped with EDAX Apollo-XL energy-dispersive X-ray spectroscopy detector. For STEM observation, 16-2-16 tartrate (0.4 mM) in water aged at 20 °C for 24 h, silica nanohelices dispersed in water and Tb^{3+} ion-doped nanosilicas (SiO_2:Tb^{3+}s) dispersed in butanol were spotted onto carbon-coated copper grids. The samples were air-dried at ambient temperature by blotting excess solution using filter paper. The sample of 16-2-16 tartrate was post-stained with osmium tetroxide using a Filgen osmium plasma coater OPC60A. For EDX measurement, SiO_2:Tb^{3+}s were pasted on a carbon tape and measured at an accelerating voltage of 30 kV without any coating.

Elemental analysis

The amount of gemini surfactant in silica nanohelices after washing with methanol was estimated by elemental analysis. The freeze-dried silica nanohelices were further dried at 120 °C for 3 h before analysis.

Excitation and emission spectral measurements

Lanthanide ion-doped nanosilicas were mounted in a powder sample cell (PSH-002, JASCO). Solid-state excitation and emission spectra were measured at ambient temperature (25 °C) with a JASCO FP-6600 spectrofluorometer equipped with an integrating sphere (ISF-513, JASCO) and a 422 nm cut-off filter (LU0422, Asahi Spectra Co., Ltd.) in front of the detector.

Electronic circular dichroism, linear dichroism and ultraviolet absorption spectral measurements

Lanthanide ion-doped nanosilicas and silica nanohelices were grinded and mounted in a powder sample holder. Diffuse reflectance electronic circular dichroism (ECD), linear dichroism (LD) and ultraviolet (UV) absorption spectra were measured at ambient temperature (25 °C) with a JASCO J-820 spectropolarimeter equipped with a solid-state CD measurement unit with a barium sulfate-coated integrating sphere (DRCD-466L) and LD attachment (LD-403).

Circularly polarized luminescence spectral measurement

Ground SiO_2:Tb^{3+}s were mounted in a 0.01 cm path length quartz cell. Circularly polarized luminescence (CPL) spectral measurement was performed at ambient temperature (25 °C) using a JASCO CPL-300 spectrofluoropolarimeter.

Thermal gravimetric analysis

Thermal gravimetric analysis (TGA) was performed with an STA7200 thermal analysis system (Hitachi High-Tech Science). Silica nanohelix after immersing in terbium(III) acetate aqueous solution was placed in a Pt open pan and scanned in synthetic air using a heating rate of 10 °C min^{-1} from room temperature to 1100 °C.

Fourier transform infrared spectral measurement

Fourier transform infrared (FTIR) spectra of SiO_2:Tb^{3+}s were measured at ambient temperature (25 °C) with a JASCO FT/IR-6300 FTIR spectrometer equipped with a JASCO ATR Pro450-S.

High resolution transmission electron microscopy observation and fast Fourier transform analysis

High resolution transmission electron microscopy (HRTEM) observation was made with a spherical-aberration-corrected transmission electron microscope (JEM-2200FS + CETCOR, JEOL). SiO_2:Tb^{3+}s dispersed in butanol were spotted onto carbon-coated copper grids. The samples were air-dried at ambient temperature by blotting excess solution using filter paper. Fast Fourier transform analysis was carried out by using Image J.

Supplementary figures

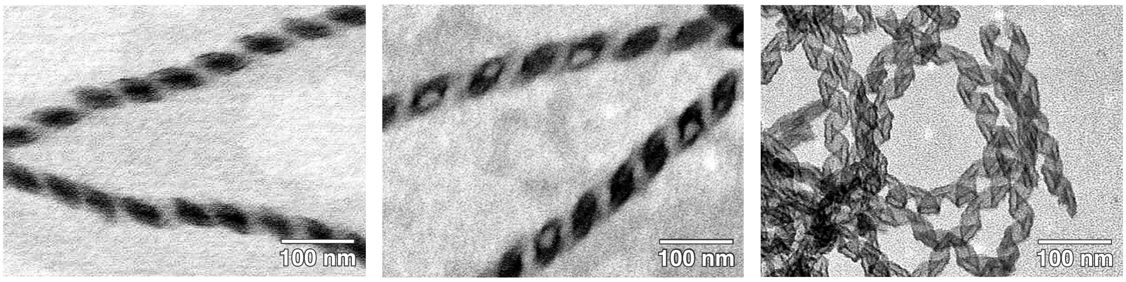
(a) 16-2-16 L-tartrate assemblies

(b) 16-2-16 D-tartrate assemblies

(c) L-SiO$_2$:Tb^{3+} calcined at 600 °C

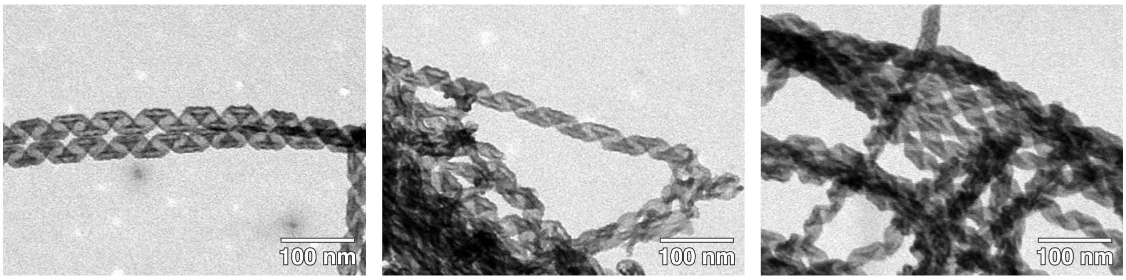
(d) L-SiO$_2$:Tb^{3+} calcined at 700 °C

(e) L-SiO$_2$:Tb^{3+} calcined at 800 °C

(f) L-SiO$_2$:Tb^{3+} calcined at 1000 °C

Fig. S1 STEM images of (a) 16-2-16 L-tartrate and (b) 16-2-16 D-tartrate self-assemblies in the cast film prepared from a 0.4 mM aqueous solution post-stained with osmium tetroxide and L-SiO$_2$:Tb^{3+} calcined at (c) 600, (d) 700, (e) 800 and (f) 1000 °C.

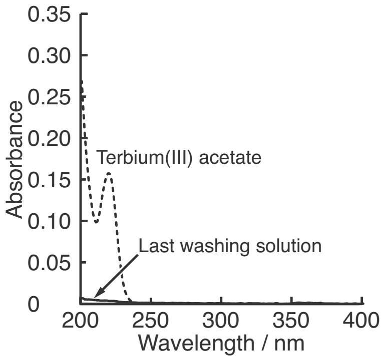

Fig. S2 UV absorption spectra of terbium(III) acetate aqueous solution at 0.5 mM and the last washing solution (water) for silica nanohelices prepared from 16-2-16 L-tartrate after the immersion process; temperature: 20 °C, path length: 1.0 cm.

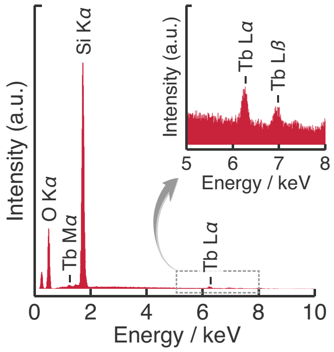

Fig. S3 EDX spectrum of L-SiO$_2$:Tb^{3+} calcined at 900 °C.

Table S1 Concentrations of Tb and Eu doped in nanosilicas estimated from EDX spectroscopy and inductively coupled plasma (ICP) analysis; calcination temperature: 600–1200 °C, [terbium(III) acetate] in immersion process: 0.2, 2 and 20 mM.

Sample	lanthanide concentration / at% (from EDX spectroscopy)	lanthanide concentration / at% (from ICP analysis)
L-SiO$_2$:Tb^{3+} (600 °C, 20 mM)	0.31	0.22
L-SiO$_2$:Tb^{3+} (700 °C, 20 mM)	0.30	0.31
L-SiO$_2$:Tb^{3+} (800 °C, 20 mM)	0.31	0.32
L-SiO$_2$:Tb^{3+} (900 °C, 20 mM)	0.30	0.22
D-SiO$_2$:Tb^{3+} (900 °C, 20 mM)	0.32	0.23
L-SiO$_2$:Tb^{3+} (1000 °C, 20 mM)	0.30	0.22
L-SiO$_2$:Tb^{3+} (1100 °C, 20 mM)	0.30	0.29
L-SiO$_2$:Tb^{3+} (1200 °C, 20 mM)	0.35	0.23
L-SiO$_2$:Tb^{3+} (uncalcined, 20 mM)	0.32	0.28
D-SiO$_2$:Tb^{3+} (uncalcined, 20 mM)	0.33	—
L-SiO$_2$:Tb^{3+} (900 °C, 2 mM)	—	0.05
L-SiO$_2$:Tb^{3+} (900 °C, 0.2 mM)	—	0.006
Twisted L-SiO$_2$:Tb^{3+} (900 °C, 20 mM)	0.37	0.66
Twisted D-SiO$_2$:Tb^{3+} (900 °C, 20 mM)	0.40	—
L-SiO$_2$:Eu^{3+} (900 °C, 20 mM)	0.32	—
D-SiO$_2$:Eu^{3+} (900 °C, 20 mM)	0.35	—

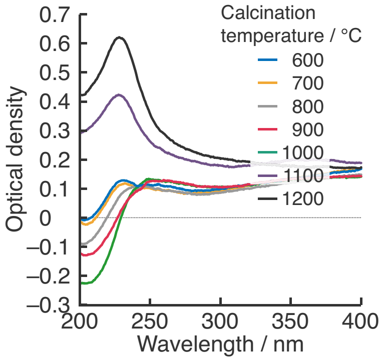

Fig. S4 UV absorption spectra of L-SiO_2:Tb^{3+} calcined at different temperatures (600–1200 °C); measurement temperature: 25 °C.

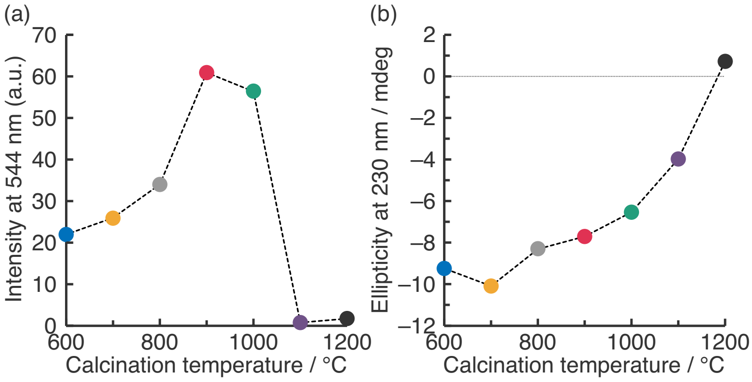

Fig. S5 Variations of (a) emission intensity at 544 nm and (b) ellipticity at 232 nm of L-SiO_2:Tb^{3+}s calcined at different temperatures (600–1200 °C). These data were taken from Fig. 3b and c, respectively.

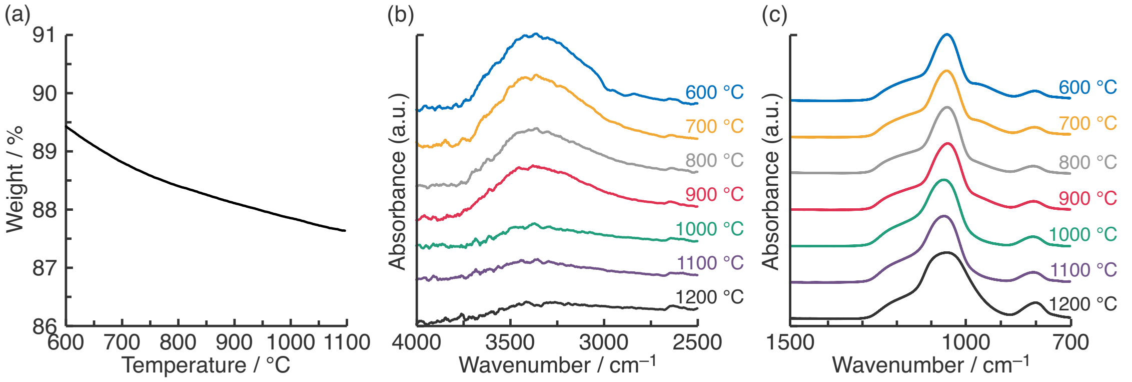

Fig. S6 (a) TGA thermogram of silica nanohelix after immersing in terbium(III) acetate aqueous solution before calcination; heating rate: 10 °C min^{-1}. (b) and (c) Normalized FTIR spectra of L-SiO_2:Tb^{3+} calcined at different temperature (600–1200 °C).

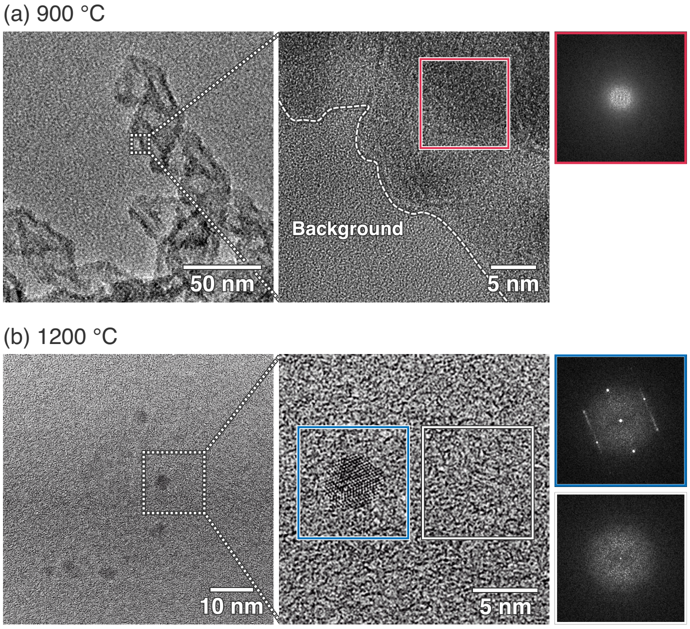

Fig. S7 HRTEM images (left and middle) and FFT patterns (right) of L-SiO_2:Tb^{3+} calcinated at (a) 900 and (b) 1200 °C. White dotted line in (a, middle) indicates the boundary between helical object and background. FFT pattern in (a, right) was taken from red square part in (a, middle). Two FFT patterns in (b, right) were taken from blue and white square parts in (b, middle).

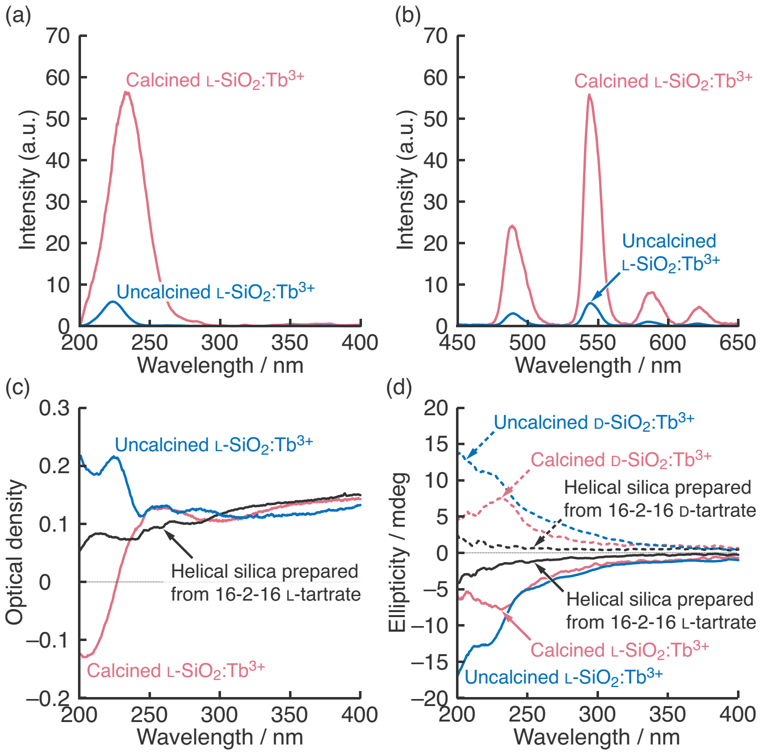

Fig. S8 (a) Excitation, (b) emission, (c) UV absorption and (d) ECD spectra of helical silica without any doping calcined at 900 °C and helical SiO_2:Tb^{3+}s uncalcined and calcined at 900 °C; measurement temperature: 25 °C, emission wavelength for (a): 544 nm, excitation wavelength for (b): 230 nm.

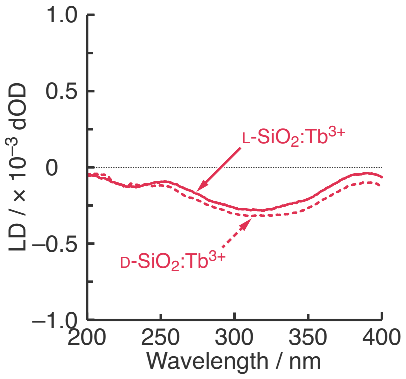

Fig. S9 LD spectra of L- and D-SiO_2:Tb^{3+} calcined at 900 °C; measurement temperature: 25 °C.

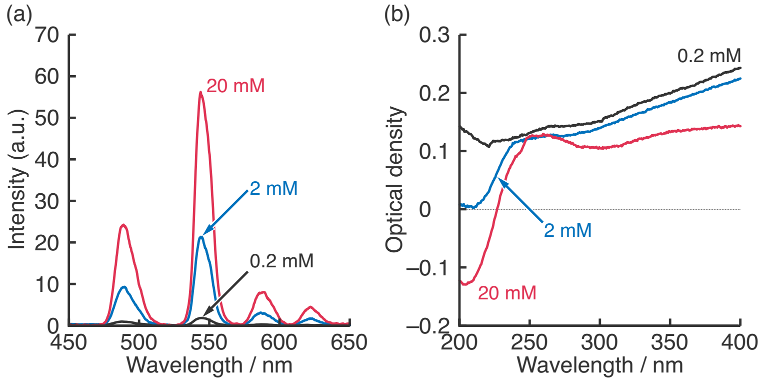

Fig. S10 (a) Emission and (b) UV absorption spectra of L-SiO_2:Tb^{3+}s calcined at 900 °C which were prepared using 20, 2 and 0.2 mM terbium(III) acetate aqueous solution in the immersion process; measurement temperature: 25 °C, excitation wavelength for (a): 230 nm.

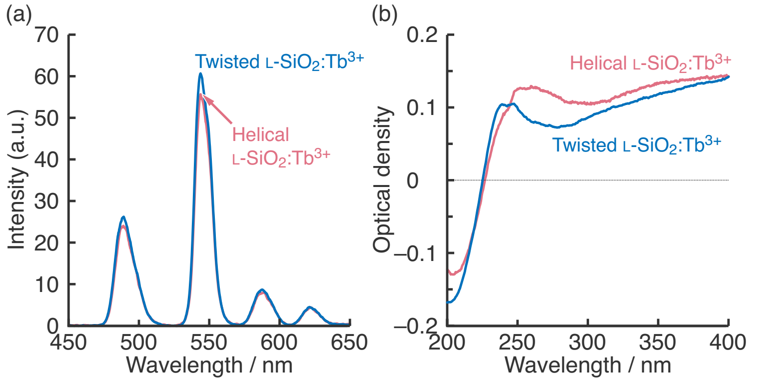

Fig. S11 (a) Emission and (b) UV absorption spectra of twisted and helical L-SiO_2:Tb^{3+} calcined at 900 °C; measurement temperature: 25 °C, excitation wavelength for (a): 230 nm.

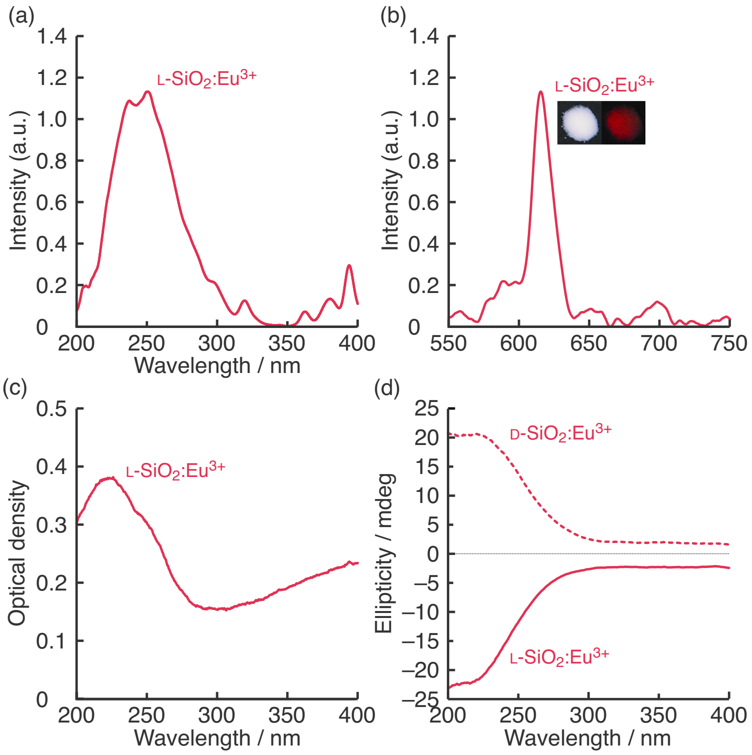

Fig. S12 (a) Excitation, (b) emission, (c) UV absorption and (d) ECD spectra of $SiO_2:Eu^{3+}$ calcined at 900 °C; measurement temperature: 25 °C, emission wavelength for (a): 616 nm, excitation wavelength for (b): 254 nm. Insets in (b) show pictures of L-$SiO_2:Eu^{3+}$ in daylight (left) and under 254 nm UV light in the dark (right).

Author contributions

All authors discussed the results, commented on the manuscript and contributed to the interpretation of the data. The cationic gemini surfactants were synthesized by T. Harada and N. Ryu. The silica nanohelices, SiO_2:Tb^{3+}s and SiO_2:Eu^{3+}s were prepared by T. Harada and H. Yanagita. STEM images were taken and EDX spectra were measured by T. Harada and H. Yanagita. Excitation, emission, ECD, LD and UV absorption spectral measurements were carried out by T. Harada and H. Yanagita. CPL spectral measurements were carried out by N. Ryu and Y. Okazaki. TGA and FTIR spectra were measured by T. Harada and S. Nagaoka. HRTEM observation and FFT analysis were carried out by Y. Okazaki. N. Ryu, H. Ihara and R. Oda designed the study. S. Nagaoka, M. Takafuji and Y. Kuwahara were involved in study design. T. Harada and N. Ryu drafted the manuscript and Y. Okazaki, M. Takafuji, H. Ihara and R. Oda assisted in the preparation of the manuscript.